IONIZATION FRONT ACCELERATOR*

C. L. Olson
Sandia National Laboratories
Albuquerque, NM 87185

Abstract

The ionization front accelerator (IFA) is the first controlled collective accelerator powered by an intense relativistic electron beam to demonstrate particle acceleration with a high acceleration gradient. Here the IFA concept is reviewed, results of second generation accelerator experiments are summarized, and an analysis for future IFA development is presented.

Concept

The ionization front accelerator (IFA) is a collective ion accelerator in which the large space charge field at the head of an intense relativistic electron beam (IREB) is controlled by a laser to produce high gradient particle acceleration.[1,2] In the basic concept, as shown in Fig. 1(a), an IREB is injected into a metallic drift tube filled with a special working gas. The pressure of the working gas is chosen low enough so that the IREB does not significantly ionize it before a photoionizing laser beam does, that is injected through a window along the side of the drift tube. As the laser beam is swept, a plasma of density n_p is created with $n_p \approx n_e$ where n_e is the IREB density.[p] As the plasma electrons are expelled by the IREB's space charge field, an ion background density n_{pi} is left that permits the IREB to propagate in a charge neutralized state. Ions (e.g., from an ion source gas mixed with the working gas) are trapped and accelerated in the strong potential well at the IREB head.

Key features of the IFA include a high acceleration gradient, a relatively low laser energy requirement, and a moderately high efficiency. The peak axial electric field that can be created is

$$E_z = 2\pi n_e e r_b \qquad (1)$$

where r_b is the IREB radius and e is the electron charge.[b] Fields exceeding 100 MV/m are already routinely available; fields of 1 GV/m and higher should be attainable. The energies of the laser, ions, and IREB are ordered as

$$\mathcal{E}_{laser} \ll \mathcal{E}_{ions} < \mathcal{E}_{IREB} \qquad (2)$$

so that a very small amount of laser energy is used to control a large amount of pulsed power IREB energy. Theoretical conversion efficiencies of IREB energy to ion energy are relatively high (e.g., 32% for 300 MeV protons).[1]

IFA scenarios are given in Fig. 1(a), (b), (c) that produce phase velocities ranging from zero up to the speed of light c. These are divided into three cases as follows:

(a)	non-relativistic case	$0 \le \beta_{iz} < \beta_{ez}$
(b)	transition case	$\beta_{ez} \lesssim \beta_{iz} \lesssim 1$
(c)	relativistic case	$\beta_{iz} \approx 1$

where $\beta_{iz}c$ is the ion axial velocity and $\beta_{ez}c$ is the IREB axial velocity. Note that because of the electron's betatron oscillations in the IREB's self fields, we have $\beta_{ez} < \beta_e$ where $\beta_e c$ is the injected electron velocity.[e] For cases (b) and (c) where β_{iz} exceeds β_{ez}, the IREB is made to pre-propagate ahead of the ion bunch so the laser sweep velocity can exceed $\beta_{ez}c$.[1] This is done by creating a weak preformed plasma with $\gamma_e^{-2} < f_e \ll 1$, or by using an axial magnetic field B_z. Here $\gamma_e = [1 - \beta_e^2]^{-1/2}$ and $f_e = n_{pi}/n_e$. For case (c), a short laser pulse (typically $\lesssim$ 30 ps for r_b = 1 cm) is injected co-linearly with the IREB. Note that case (c) can in principle be used to attain unlimited ion energies.

Demonstration Experiments

Two complete IFA systems, IFA-1[3] and IFA-2[4], have been built and tested. IFA-1 used a 0.6 MeV IREB and had a 10 cm acceleration length; IFA-2 used a 1 MeV IREB and had a 30 cm acceleration length. Both systems used Cs as the working gas and two-step laser photoionization with excitation at 852.1 nm and photoionization from the excited state at 347 nm (IFA-1) or 308 nm (IFA-2). The advantage of the two-step process is that the cross section for photoionization from the excited state is about 50 times larger than the cross section for photoionization from the ground state. Synchronization of the lasers with the IREB was needed to within 1 ns. Self-breakdown oil Blumlein switches on IFA-1 had a 1-σ jitter of 6 ns; laser-triggered gas Blumlein switches on IFA-2 reduced the 1-σ jitter to ~ 1 ns. Key results of the IFA-1 and IFA-2 experiments are as follows:[3,4]

1. Cs was shown to be a feasible working gas at a reduced pressure of 30 microns (i.e., a neutral density of 1.0×10^{15} cm^{-3}). In IFA-1, the excitation laser was swept while the kicker laser was on. In IFA-2, the entire Cs volume was excited, and then the kicker laser was swept. Both schemes work.
2. An accurately-controlled fast laser sweep was demonstrated with two different methods. In IFA-1, a passive light pipe array swept the dye laser exciter beam quadratically in time. In IFA-2, an electro-optic crystal deflector swept the XeCl laser kicker beam quadratically in time (typically 30 cm in 20 ns). Both sweep methods work.
3. Laser-controlled motion of the IREB beam front was demonstrated on both IFA-1 and IFA-2. Programmed sweep motion was observed with streak photography. Controlled phase velocities $\beta_\phi c$ programmed for β_ϕ = 0 - 0.07, 0 - 0.1, and 0 - 0.14 were demonstrated.
4. A small amount of laser energy was shown to control a large amount of IREB energy in IFA-2 experiments. Specifically, it was shown that

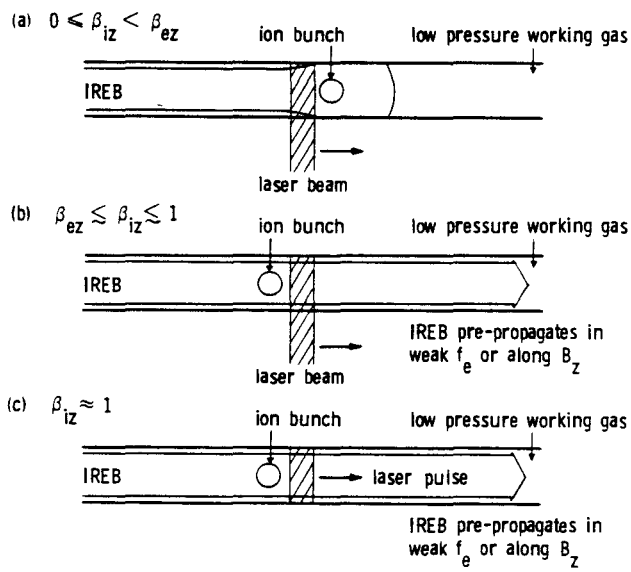

Fig. 1. Ionization Front Accelerator (IFA).

*Supported by U.S. Department of Energy under contract DE AC04-76-DP 00789.

0.001 J/cm^2 of dye laser and 0.0005 J/cm^2 of XeCl laser could control 1,000 J of IREB energy.

5. Ion acceleration at the programmed phase velocity was demonstrated on IFA-2. 5 MeV H^+, 10 MeV D^+, and 20 MeV He^{++} ions were produced (each originated from the appropriate ion source gas). The D^+ and He^{++} ion data demonstrated that particle acceleration with controlled fields of 33 MV/m over 30 cm had been achieved with a controlled collective accelerator using an IREB for the first time.

Scaling for Future Development

Previously, scaling calculations were made for the IFA case of Fig. 1(a), including efficiency estimates and seven limits to the beam front velocity.[1] Here we consider scaling to higher energies, and we examine radial focus, adiabatic cooling and damping of transverse oscillations, axial energy spread, secondary electron escape, gas scattering, and potential instabilities. Following this, we present an IFA design chart.

Radial Focus

Using the two-mass approximation, the radial force equation for an ion in the potential well is

$$\gamma_i AM_p \ddot{r} = -Ze2I_e(\beta_{ez} cr_b)^{-1}\{(1-f_e)-\beta_{iz}\beta_{ez}(1-f_m)\}r/r_b \quad (3)$$

where $\gamma_i = [1-\beta_i^2]^{-1/2}$, M_p is the proton mass, A is the atomic number, $+Ze$ is the ion charge, I_e is the IREB current, f_e is the fractional charge neutralization, and f_m is the fractional magnetic neutralization. For the IFA case of Fig. 1(a), with $f_e = f_m = 0$ in the well region, we have

$$\gamma_i AM_p \ddot{r} = -Ze2I_e(\beta_{ez} cr_b)^{-1}\{1-\beta_{iz}\beta_{ez}\}r/r_b \quad (4)$$

As the ion accelerates, the transverse mass increases ($\sim \gamma_i$) and the radial focusing force decreases ($\sim 1-\beta_{iz}\beta_{ez}$) but always remains focusing.

For the IFA cases of Figs. 1(b) and (c) with a weak preformed plasma and $\beta_{iz} > \beta_{ez}$, the radial force will be focusing or defocusing depending on the radial distribution of the preformed plasma. If the plasma is uniform with $\gamma_e^{-2} < f_e \ll 1$, then the electrons will focus and the ions will defocus. However, it is possible to focus both the electrons and the ions if the preformed plasma is created with an annular laser beam. For example, if $n_p = 0$ in an inner core (e.g., $0 \le r/r_b \le 0.5$) and $n_p \neq 0$ in an outer annulus (e.g., $0.5 \le r/r_b \le 1$), then the ions contained within the inner core will have $f_e = 0$ and will always focus, and the electrons will traverse both areas and will always be focused in the outer annulus. The plasma ion annulus will be attracted inward, but the IFA sweep can occur before the ion annulus contracts significantly.

Adiabatic Cooling and Damping

The radial force Eq. (4) is an harmonic oscillator equation with slowly varying parameters (γ_i, β_i). For the adiabatic case, the motion maintains constancy of the action angle variable $\mathcal{E}/\omega$ where $\mathcal{E}$ is the local oscillation energy and ω is the local oscillation frequency. The resultant solution of (4) is

$$r = r_o \frac{1}{\gamma_i^{1/4}(1-\beta_{iz}\beta_{ez})^{1/4}} \cos \int_o^t \left[\frac{K(1-\beta_{iz}\beta_{ez})}{\gamma_i}\right]^{1/2} dt \quad (5)$$

where $K = Ze2I_e(\beta_{ez} cr_b^2 AM_p)^{-1}$. It follows that

$$\left.\begin{aligned} r &\sim \gamma_i^{-1/4}(1-\beta_{iz}\beta_{ez})^{-1/4} \quad \text{(damping)} \\ \dot{r} &\sim \gamma_i^{-3/4}(1-\beta_{iz}\beta_{ez})^{+1/4} \quad \text{(cooling)} \end{aligned}\right\} \quad (6)$$

The transverse emittance then scales as

$$\varepsilon_\perp = \pi r(\gamma_i AM_p \dot{r})/(\beta_i\gamma_i AM_p c) \sim (\beta_i\gamma_i)^{-1} \quad (7)$$

which improves as the ion energy increases.

Axial Energy Spread

Following a similar procedure for the axial oscillations, and using the two-mass approximation (so the longitudinal oscillating mass is $\gamma_i^3 AM_p$), we find the adiabatic harmonic oscillator equation for the axial (z) motion yields

$$\left.\begin{aligned} z &\sim \gamma_i^{-3/4} \quad \text{(damping)} \\ \dot{z} &\sim \gamma_i^{-9/4} \quad \text{(cooling)} \end{aligned}\right\} \quad (8)$$

The longitudinal emittance and the axial ion energy spread then scale as

$$\varepsilon_\parallel = \pi z(\gamma_i^3 AM_p \dot{z})/(\beta_i\gamma_i AM_p c) \sim (\beta_i\gamma_i)^{-1} \quad (9)$$

$$\Delta\mathcal{E}_i/\mathcal{E}_i = (e\phi_o/\mathcal{E}_i)\gamma_i^{-3/2} \quad (10)$$

where $e\phi_o$ is the initial potential well depth. Both $\varepsilon_\parallel$ and $\Delta\mathcal{E}_i/\mathcal{E}_i$ improve as the ion energy increases.

Secondary Electron Escape

As plasma is created by laser photoionization near the potential well, it is assumed that the plasma electrons will be expelled to the walls at radius R ($R \approx r_b$) essentially instantaneously until $f_e = 1$. In reality, expulsion by the radial electric field E_r is complicated by the presence of the beam's self magnetic field B_θ which, if large enough, can tend to trap the secondaries. If trapped, the secondaries will drift toward the beam front with trajectories that resemble $E_r \times B_\theta$ drift trajectories. Fortunately there is also an axial E_z near the potential well that causes an $E_z \times B_\theta$ drift in the outward radial direction, that does cause the secondaries to escape. These drifts are given approximately by:

$$\text{axial drift:} \quad v_z \approx (E_r/B_\theta)c \approx (1-f_e)\,\beta_{ez}^{-1}\,c \quad (11a)$$

$$\text{radial drift:} \quad v_r \approx (E_z/B_\theta)c \approx (r_b/\Delta z)\,\beta_{ez}^{-1}\,c \quad (11b)$$

where Δz is the axial gradient length over which the potential drops. Initially, $E_r > B_\theta$, and the secondaries do directly escape radially. As f_e exceeds γ_e^{-2}, then trapping can begin if the height of the drift trajectory is contained within the IREB. The cyclotron radius of a secondary electron at the beam edge using (11a) for the drift velocity is

$$r_{ce} = r_b(1-f_e)\,\beta_{ez}^{-1}(mc^3/e)/(2I_e) \quad (12)$$

This shows that for large I_e, and/or as f_e approaches 1, trapping occurs with the axial drift (11a) and secondaries will not escape directly in the net E_r. However, they will escape by the radial drift (11b).

Gas Scattering

Since the IFA requires a background working gas, it is of interest to see if the accelerated ion beam will be scattered significantly by the gas. The mean square angle of the Gaussian multiple scattering distribution is[5]

$$\langle\theta^2\rangle = 4\pi n_g(2Z_g e^2)^2(\beta_i^2\gamma_i AM_p c^2)^{-2} \cdot[\ln(210\, Z_g^{-1/3})]\, L \quad (13)$$

where g refers to the working gas and L is the ion path length. For proton acceleration with Cs as the working gas ($Z = 55$, $n_g = 1.0 \times 10^{15}$ cm^{-3}), this is

$$\langle\theta^2\rangle = 1.4 \times 10^{-11}\,(\beta_i^{-4}\gamma_i^{-2})\, L(\text{cm}) \quad (14)$$

In an IFA with 100 MV/m accelerating fields, proton acceleration to 1 MeV ($\beta = 0.046$) occurs in 1 cm, and to 100 MeV ($\beta = 0.43$) in 100 cm. Because acceleration to high β occurs so quickly, scattering effects as given by (14) appear to be negligible. Also once relativistic energies are reached ($\gamma_i \gtrsim 2$) scattering effects become even more negligible.

Potential Instabilities

We have examined several possible instabilities, and we can present only a brief summary here. The e-i two-stream instability for IREB electrons and plasma ions has a 2-D current threshold[1] at $I_e = \gamma_e(\gamma_e+1)\, I_\ell$; for the IFA, $I_e \lesssim I_\ell$ typically so I_e is well below the threshold current for instability. We have also examined the e-e two-stream instability (IREB electrons, plasma electrons), return current (Buneman) instability (plasma electrons, plasma ions), filamentation instability, and resistive hose instability. For the ideal IFA ($f_e = 1$, no return current, $\sigma = 0$) none of these instabilities should even occur. For a real IFA with possible over neutralization, some of these may occur. However, for that case, we have estimated saturation effects to be small, or stabilization to occur by transverse velocity spreads or by image current wall stabilization.

IFA Design Chart

Having established from the above that scaling of the IFA to very high energies appears plausible, we present in Fig. 2 a chart to aid in designing IFA's. Here the IREB current I_e is plotted against the IREB radius r_b. If we specify $I_e \lesssim I_\ell$, then the IREB energy must be $\mathcal{E}_e \gtrsim eI_e/(\beta_{ez}c)$. In practical units, this is

$$\mathcal{E}_e(\text{eV}) \gtrsim 30\, I_e(\text{A})/\beta_{ez} \qquad (15)$$

Fig. 2 shows sets of lines giving the axial acceleration gradient E_z, the IREB current density J_e, and the number of ions $N_i = n_e r_b$ accelerated per pulse. Two constraint boundaries are also shown. The working gas depletion limit occurs when $n_e = n_g$ so the working gas, if fully ionized, can just reach $f_e = 1$. The charge exchange limit for the ion source gas requires $E/p \gtrsim 10^6$ V/cm/Torr for the initial acceleration to 100 keV. The IFA-2 operating point (1 MeV, 30 kA, $r_b = 1$ cm) is shown in the center of the figure.

Some interesting comments can be made in relation to Fig. 2. First note that fields of 1 GV/m and higher are well within the allowed parameter space. To achieve high fields at moderate currents requires small radius beams with high current densities (e.g., 16 kA in a 1 mm radius beam gives a 1 GV/m field). Also, for high fields ($E \gtrsim 1$ GV/m), Stark field ionization may be used to ionize the excited state working gas atoms; then no kicker laser is required, and only a swept dye laser exciter is needed.

Most IFA applications require ion energies of 100 MeV $\lesssim \mathcal{E}_i/A \lesssim$ 1 GeV, which can be achieved with the IFA of Fig. 1(a) with a length of 1-10 meters. For high energy physics applications, a staged IFA consisting of all three IFA cases of Fig. 1 would be used. For example, for a 1 TeV proton IFA, the three cases of Fig. 1 would be:

(a) 0 to 1 GeV	β_i = 0-0.87	γ_i = 0-2
(b) 1 GeV to 20 GeV	β_i = 0.87-0.999	γ_i = 2-22
(c) 20 GeV to 1 TeV	β_i = 0.999-0.999999	γ_i = 22-1067

For case (c), 10 meter sections at 1 GV/m are envisioned.

Conclusions

The IFA concept for $0 \lesssim \beta_i \lesssim 1$ has been discussed. Results of IFA experiments that demonstrated particle acceleration with controlled fields of 33 MV/m over 30 cm were summarized. Several scaling features of the IFA were examined, and a design chart for future IFA development was presented.

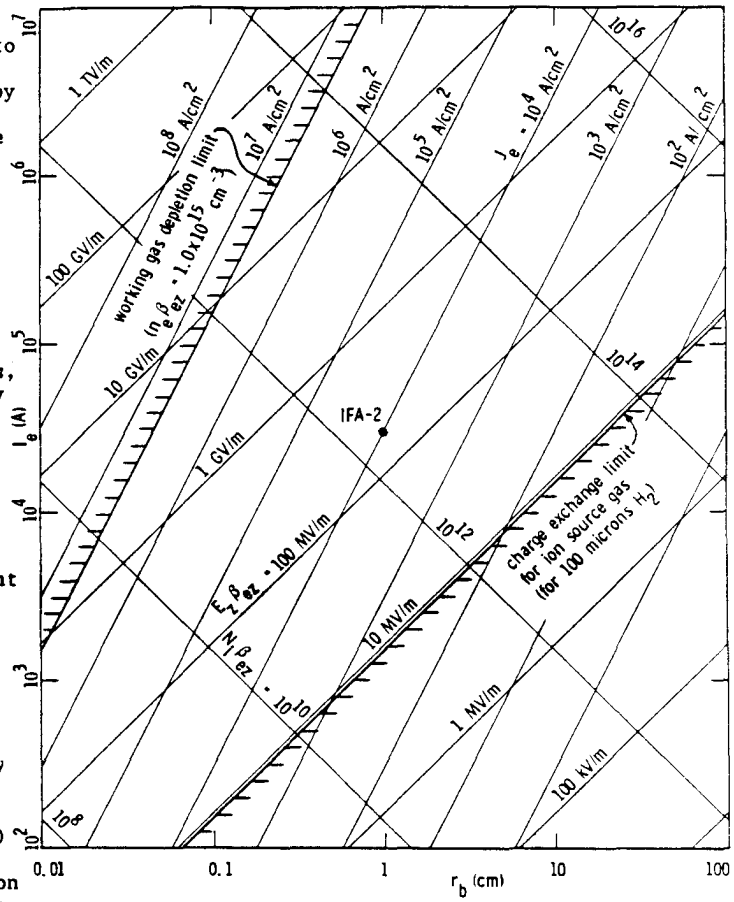

Fig. 2. IFA design space for high gradient acceleration.

Acknowledgements

IFA-1 research was supported by the Division of Nuclear Sciences, DOE, and by the Air Force Office of Scientific Research.

IFA-2 research was supported by the Division of Advanced Energy Projects, DOE and by Defense Programs, DOE.

References

1. C. L. Olson and U. Schumacher, Collective Ion Acceleration, Springer Tracts in Modern Physics, V. 84, Heidelberg: Springer-Verlag, 1979, pp. 105-116.
2. C. L. Olson, "Collective Ion Accelerator," Bull. A.P.S., 18, p. 1369, 1973; C. L. Olson, "Two New Collective Accelerator Schemes," Proc. IX Int. Conf. High Energy Accel., SLAC, May 2-7, 1974, pp. 272-276, 1974; C. L. Olson, "Ionization Front Accelerator," Proc. Int. Top. Conf. E-Beam Res. and Tech., Albuquerque, NM, Nov. 3-5, 1975, V. 2, pp. 312-333, 1974.
3. C. L. Olson, "IFA Proof of Principle Experiments," IEEE Trans. Nucl. Sci, NS-26, pp. 4231-4233, 1979.
4. C. L. Olson, C. A. Frost, E. L. Patterson, J. P. Anthes, and J. W. Poukey, "IFA-2 Collective Ion Accelerator Experiments," IEEE Trans. Nucl. Sci., NS-32, pp. 3530-3532, 1985.
5. J. D. Jackson, Classical Electrodynamics, New York: Wiley, 1963, pp. 451-459.
6. C. L. Olson, "Charge Neutralization Processes for Intense Relativistic Electron Beams in Low Pressure Neutral Gases," Phys. Rev. A, 11, pp. 288-296, 1975.